J Appl Electrochem (2009) 39:769–778
DOI 10.1007/s10800-008-9717-x

ORIGINAL PAPER

Adsorption and inhibitive corrosion properties of thiourea derivatives on cold rolled steel in 1 M $HClO_4$ solutions

O. Benali · L. Larabi · Y. Harek

Received: 27 January 2008 / Accepted: 6 November 2008 / Published online: 25 November 2008

Abstract Thiourea derivatives namely, phenylthiourea (PTU), *N*, *N*′-diphenylthiourea (DPTU) and *N*-naphtyl *N*′-phenylthiourea (NPTU) synthesised in our laboratory, were tested as inhibitors for the corrosion of cold rolled steel in 1 M $HClO_4$ using polarisation and electrochemical impedance measurements. At 30 °C, PTU and DPTU stimulated corrosion at low concentrations while addition of NPTU caused inhibition at all concentrations. The best protection (93%) was obtained by adding NPTU at 2.5×10^{-4} M. Polarisation curves showed that NPTU acted as a mixed inhibitor. The degree of surface coverage of the adsorbed inhibitors was determined by the ac impedance technique. The adsorption of NPTU on the cold rolled steel surface obeyed the Langmuir adsorption isotherm. Corrosion behaviour in the presence of NPTU at various concentrations was studied in the temperature range 20–50 °C. Both the corrosion rate of cold rolled steel and protection efficiency increased with increasing temperature. Activation energies with and without NPTU were obtained from the temperature dependence of corrosion current. The thermodynamic functions of the adsorption processes were calculated from the polarisation data and were used to analyse the inhibitor adsorption mechanism.

Keywords Thiourea derivatives · Electrochemical impedance spectroscopy · Polarisation measurements · Cold rolled steel · Inhibition corrosion · Perchloric acid · Adsorption

O. Benali
Département de biologie, centre universitaire de Saïda, 20000 Saida, Algeria

L. Larabi (✉) · Y. Harek
Département de Chimie, Faculté des sciences, Université Abou Bakr Belkaïd, 13000 Tlemcen, Algeria
e-mail: larabi_lahcene@yahoo.fr

1 Introduction

The use of inhibitors is one of the most important methods for protection of carbon steel against corrosion in acidic media. Extensive investigations on inhibitors have been carried out, especially on nitrogen- and sulphur-containing inhibitors. Substantial progress has been made in this field in recent years [1–5]. Thiourea and its derivatives have been used as good candidates of organic inhibitors for corrosion of iron and steel [6–10].

The synthesis of novel organic molecules offers different molecular structures containing several heteroatoms and substituents. Their adsorption is generally due to the formation of a film bonded to a metal surface with a physical or chemical mechanism. It has been suggested that chemisorbed molecules protect anodic areas and reduce the inherent reactivity of the metal at the sites where they are attached, whereas physisorbed molecules are attached to the metal at local cathodes and retard metal dissolution by stifling the cathodic reaction [11, 12].

In recent years, we have been involved in the development of new organic compounds as acid inhibitors. In the present work, we have synthesised the organic compounds *N*-phenylthiourea (PTU), *N*, *N*′-diphenylthiourea (DPTU) and *N*-naphtyl *N*′-phenylthiourea (NPTU) in order to study their ability to inhibit corrosion of cold rolled steel in perchloric acid. The choice of these compounds was based on molecular structure considerations. Introduction of phenyl and naphthyl groups changes the volume of the PTU molecule and hence the surface occupied when adsorbed on the metal. The effects of concentration of the

compounds on the electrochemical parameters of cold rolled steel in 1 M $HClO_4$ have been studied by three electrochemical methods: potentiodynamic polarisation curves, linear polarisation measurements and electrochemical impedance spectroscopy. The free energy, the enthalpy and entropy for the adsorption process were determined with and without NPTU. The apparent activation energies and pre-exponential factor for the dissolution process were also calculated.

2 Experimental

2.1 Materials

Cold rolled steel composed of (wt.%): C $\leq$ 0.15%, Mn $\leq$ 0.50%, P $\leq$ 0.03%, S $\leq$ 0.03%, remainder iron, was used as the working electrode for all studies.

Inhibitors were synthesised by condensation of phenyl isothiocyanate with an appropriate amine and were purified and analysed by IR and NMR spectroscopy before use. Figure 1 shows the molecular structures of the compounds labelled DPTU, NPTU and PTU. Acid solutions were prepared from AR grade $HClO_4$ (70%) in an appropriate concentration using double-distilled water.

2.2 Electrochemical measurements

Electrochemical experiments were carried out in a glass cell (CEC/TH-Radiometer) with a capacity of 500 mL. A platinum electrode and a saturated calomel electrode (SCE) were used as a counter electrode and a reference electrode, respectively. The working electrode (WE) was cut from cold rolled steel in the form of a disc and embedded in a Teflon rod with an exposed area of 0.5 cm^2. Prior to each experiment the WE was polished successively with different grades of emery paper up to 1,000, rinsed with bi-distilled water, degreased by acetone, washed thoroughly with bi-distilled water and dried at room temperature.

Electrochemical impedance spectroscopy (EIS), potentiodynamic and linear polarisation measurements were conducted in a PGZ301 potentiostat. A personal computer was used to collect and treat data with VoltaMaster 4 and Zview softwares.

The working electrode (WE) was immersed in test solution for 1 h until a steady state open-circuit potential (E_{ocp}) was reached**.** The potentiodynamic current-potential curves were plotted by changing the electrode potential automatically from -700 to -250 mV vs SCE with a scanning rate of 0.5 mV s^{-1}. The corrosion current densities were determined by Tafel extrapolation of the cathodic curves to the open circuit corrosion potentials.

The a.c. impedance measurements were performed at corrosion potentials (E_{corr}), after 1 h exposure of the WE in the solution, over a frequency range of 4 kHz–60 mHz, with a signal amplitude perturbation of 10 mV. Nyquist and Bode plots were obtained.

Polarisation resistance measurements were performed, immediately after EIS on the same electrode without any surface treatment, by applying a controlled potential scan over a small range typically $\pm$15 mV with respect to E_{corr}. The resulting current was plotted vs potential. The slope of the line at E_{corr} was taken as the polarisation resistance (R_p).

All experiments were carried out in freshly prepared solutions at constant temperature, 20, 30, 40 and 50 $\pm$ 0.1 °C using a thermostat.

The measurements were repeated to test the reproducibility of the results.

Inhibition efficiencies P % were calculated as follows:

– For potentiodynamic polarisation measurements:

$$P\ \% = \frac{I_{corr} - I'_{corr}}{I_{corr}} \times 100 \quad (1)$$

where I_{corr} and I'_{corr} are corrosion current densities without and with the inhibitor, respectively.

– For linear polarisation measurements:

$$P\ \% = \frac{R'_P - R_P}{R'_P} \times 100 \quad (2)$$

where R_P and R'_P are polarisation resistances without and with the inhibitor, respectively.

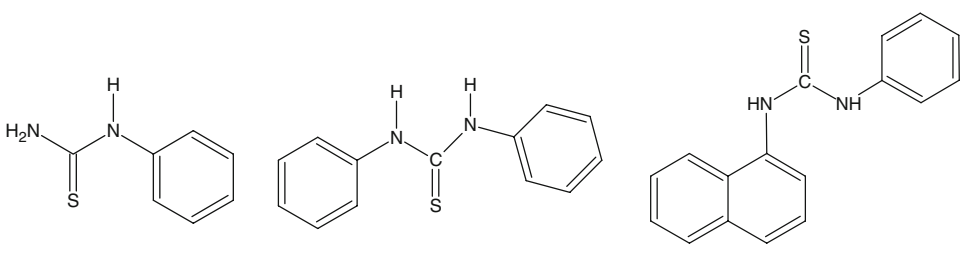

Fig. 1 Molecular structures of PTU, DPTU and NPTU

– For impedance measurements:

$$P\% = \frac{R'_t - R_t}{R'_t} \times 100 \quad (3)$$

where R_t and R'_t are charge transfer resistances without and with the inhibitor, respectively.

3 Results and discussion

3.1 Comparative study

3.1.1 Polarisation curves

Figures 2, 3, 4 depict the anodic and cathodic polarisation curves recorded on cold rolled steel in 1 M $HClO_4$ with and without addition of PTU, DPTU and NPTU at 30 °C. DPTU and PTU stimulated corrosion at low concentrations by accelerating the anodic reactions.

The electrochemical parameters derived from the polarisation curves at different concentrations are given in Table 1. PTU and DPTU acted as corrosion stimulators and the acceleration of corrosion of cold rolled steel was larger at lower concentrations. This indicated that the PTU and DPTU compounds produced a catalytic effect on the rate of steel dissolution in 1 M $HClO_4$. This can be explained as follows: some of the organic sulphur-containing molecules adsorbed on the surface of steel may decompose and produce H_2S which accelerates the corrosion of steels in acid solutions [13–15]. On the other hand, these molecules can chemisorb on steel, protect the metal surface and therefore inhibit corrosion [16, 17]. This is called the covering effect. Thus, when the phenylthiourea or diphenylthiourea concentration in the solution is fairly low, the surface coverage

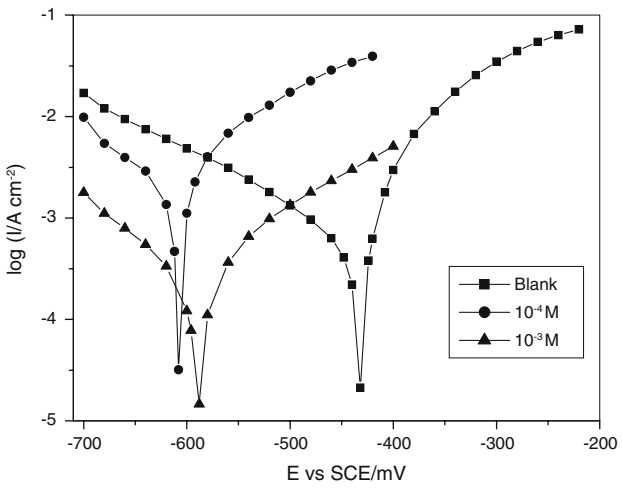

Fig. 2 Potentiodynamic polarisation curves for cold rolled steel in 1 M $HClO_4$ with and without PTU at 30 °C

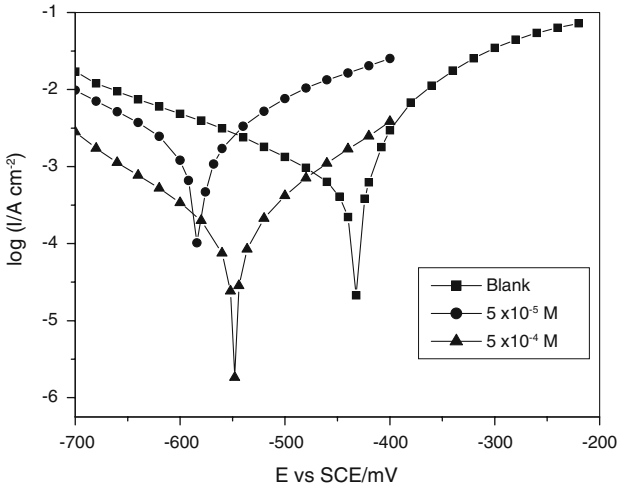

Fig. 3 Potentiodynamic polarisation curves for cold rolled steel in 1 M $HClO_4$ with and without DPTU at 30 °C

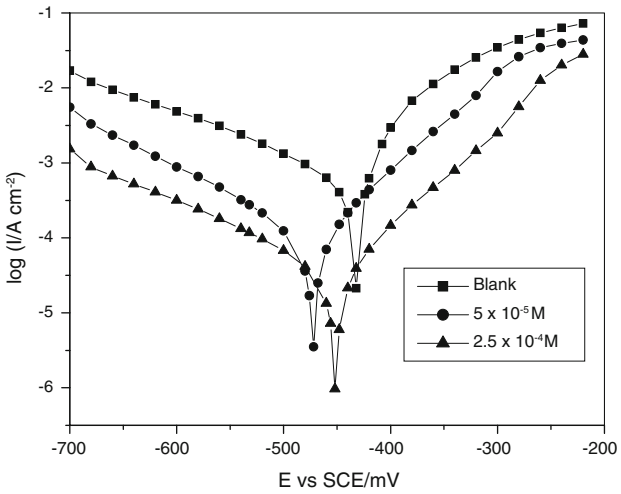

Fig. 4 Potentiodynamic polarisation curves for cold rolled steel in 1 M $HClO_4$ with and without NPTU at 30 °C

of the adsorbed molecules is too low to produce an obvious covering effect on the corrosion of steel. Moreover, it is known that even a low amount of H_2S can speed up the corrosion of steel by chemisorption on active sites and catalysing the anodic dissolution and hydrogen evolution reaction [18, 19]. Therefore, if the concentration of DPTU or PTU in the solution is low, the corrosion of cold rolled steel is accelerated by the H_2S from PTU and DPTU. Conversely, if the concentration of PTU and DPTU is higher, the surface coverage of adsorbed molecules is enhanced and a high surface coverage is reached [20]. This results in a decrease in current and corrosion rate. According to Oldham [21] the catalytic effect of these compounds may be due to changes in the oxidation state of the sulphur atoms. These atoms are easily oxidised in acid solutions making the inhibiting effect uncertain.

Table 1 Electrochemical parameters and the corresponding corrosion inhibition efficiencies for the corrosion of cold rolled steel in 1 M $HClO_4$ containing different concentrations of NPTU, DPTU and PTU at 303 K

	C (M)	$-E_{corr}$ vs SCE (mV)	I_{corr} (μA cm^{-2})	b_c (mV dec^{-1})	R_p (Ω cm^2)	P_{Icorr} (%)	P_R (%)
Blank		432	489	153	63	–	–
NPTU	5×10^{-5}	468	112	145	230	77.1	72.6
	7.5×10^{-5}	452	57	159	372	88.3	83.1
	1×10^{-4}	460	38	152	442	92.2	85.7
	2.5×10^{-4}	452	35	152	892	92.8	92.9
DPTU	5×10^{-5}	584	1,585	157	14	−69.1	−77.8
	1×10^{-4}	572	830	155	36	−41.1	−42.8
	2×10^{-4}	588	521	157	48	−06.1	−23.8
	5×10^{-4}	548	251	130	143	48.7	55.9
PTU	1×10^{-4}	612	1,841	152	10.2	−73.4	−83.8
	2.5×10^{-4}	610	1,000	125	25.4	−51.1	−59.7
	5×10^{-4}	608	759	120	42.2	−35.6	−33.0
	1×10^{-3}	580	355	135	83.9	27.4	24.9

Conversely, NPTU hinders acid attack on steel. The polarisation curves show that this inhibitor does not affect the cathodic slopes (b_c). This indicates that addition of NPTU does not modify the mechanism of the proton discharge reaction. Figure 4 also shows that NPTU exhibits both cathodic and anodic inhibition effects but the cathode is preferentially polarised. It should be mentioned that the anodic branch of the polarisation curve has a relatively small linear Tafel region, which becomes wider as the inhibitor concentration increases. For this reason, the current densities were determined by extrapolation of only the cathodic Tafel lines to the corrosion potential.

A number of significant kinetic parameters are listed in Table 1. As the concentration increased inhibitor efficiency also increased. This indicates that NPTU does not decompose in 1 M $HClO_4$. The stabilising effect that from substitution of phenyl by naphthyl group indicates rearrangement of charge densities inside the molecule giving corrosion inhibition by NPTU at all concentrations. Below 10^{-5} M, NPTU stimulates corrosion.

The linear polarisation technique was performed in 1 M $HClO_4$ with different concentrations of PTU, DPTU and NPTU. The corresponding polarisation resistances (R_p) of cold rolled steel with and without the inhibitors are also given in Table 1. It is clear that R_p increases with increasing inhibitor concentration. Percentage inhibition (P %) was calculated from R_p and is given in Table 1. P % increases with concentration of NPTU reaching 92.9 at 2.5×10^{-4} M. PTU and DPTU also stimulated corrosion up to 2×10^{-4} M for DPTU and 5×10^{-4} M for PTU.

3.1.2 Electrochemical impedance spectroscopy (EIS)

The corrosion behaviour of cold rolled steel with and without PTU, DPTU and NPTU was investigated by EIS at 30 °C after 1 h immersion in 1 M $HClO_4$. Typical sets of Nyquist plots are shown in Figs. 5, 6, 7. They exhibit one semicircle, with centre lying under the abscissa. These curves show significant differences but the impedance spectra for cold rolled steel have a similar shape at any concentration of the compounds. The emergence of one semicircle in the impedance diagrams was common to all compounds. To describe the observed depression of the capacitive semicircle, it is useful to replace the capacitor by an element which has frequency dispersion, like the constant phase element (CPE). The constant phase element is a frequency dependent element and is related to surface roughness, impurities or dislocations [22–25]. The impedance of CPE varies with frequency according to the equation [22, 26, 27]:

$$Z_{CPE} = Q^{-1}(j\omega)^{-n} \quad (4)$$

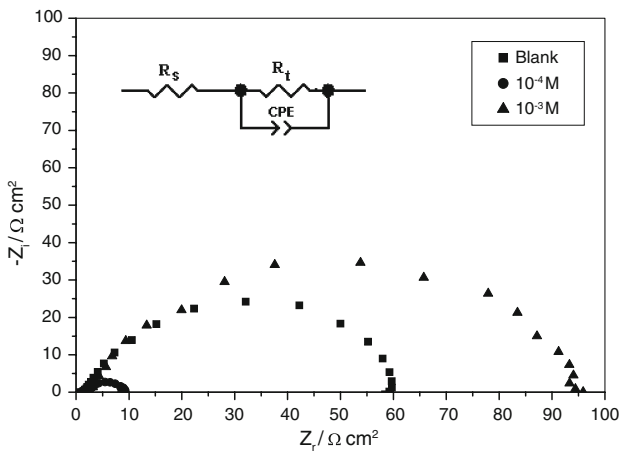

Fig. 5 Nyquist plots for cold rolled steel in 1 M $HClO_4$ with and without PTU at 30 °C. Inset shows the equivalent circuit of the impedance spectra

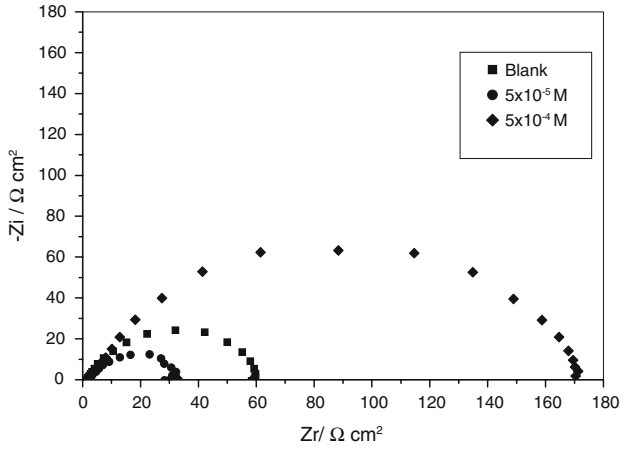

Fig. 6 Nyquist plots for cold rolled steel in 1 M $HClO_4$ with and without DPTU at 30 °C

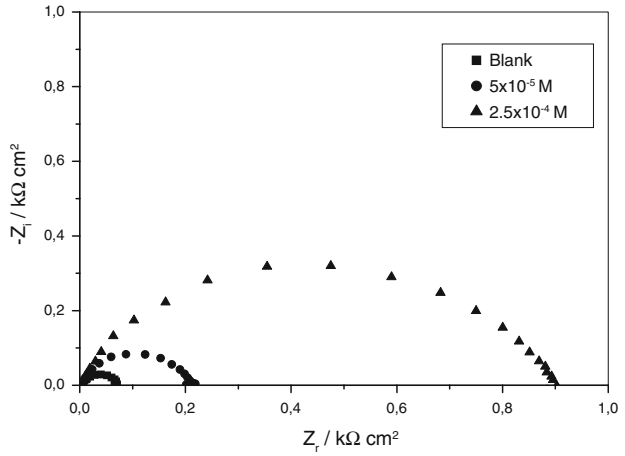

Fig. 7 Nyquist plots for cold rolled steel in 1 M $HClO_4$ with and without NPTU at 30 °C

where Q is a proportionality constant and n an exponent related to the phase shift. The above equation provides information on the extent of departure from ideal capacitance behaviour. Its value differentiates between an ideal capacitor ($n = 1$) and a CPE ($n < 1$). Values of n can serve as a measure of surface heterogeneity [22, 23, 28]. The equivalent circuit model employed for these systems is presented as an inset in Fig. 5.

The resistance R_s is that of the solution while R_t reflects the charge transfer resistance and CPE has the meaning of a frequency distributed double-layer capacitance.

Fitting parameters for the corrosion of cold rolled steel in 1 M $HClO_4$ with and without PTU, DPTU and NPTU are given in Table 2. There is good agreement with the experiments and the error does not exceed 2%**.** Some of the fitted curves are given in Fig. 8. It is seen that this model describes the experimental results very well. This model is confirmed by the Bode diagrams which show one phase angle maximum (Fig. 9).

The presence of DPTU and PTU enhanced the corrosion of cold rolled steel at different concentrations up to 2×10^{-4} and 5×10^{-4} M, respectively. This is clearly shown in the impedance experiments. High values of C_{dl} and low values of R_t are obtained for 1 M $HClO_4$ in the presence of these compound. The exponent n is higher in the presence of the compounds compared to 1 M $HClO_4$ (0.85). This shows that the stimulators contribute to lower the surface heterogeneity, presumably due to better dissolution of most active surface sites [29]. The results in Table 2 indicate that R_t increases with increasing NPTU concentration, but C_{dl} tends to decrease. The largest effect is observed at 2.5×10^{-4} M, which gives an R_t value of 881 Ω cm^2. The decrease in C_{dl} is due to adsorption of NPTU on the metallic surface. The observed decrease in n in the presence of NPTU can be explained by enhancement in the surface heterogeneity due to adsorption of inhibitor on most active desorption sites [23]. On the other hand, the excellent behaviour of NPTU previously indicated in the potentiodynamic polarisation measurements is confirmed.

Note that capacitance was calculated from Q and R_t using the equation [30, 31]:

$$Q = \frac{(CR_t)^n}{R_t} \tag{5}$$

3.2 Detailed study of NPTU

3.2.1 Kinetic parameters

The change in the rate of the corrosion process with temperature was studied in 1 M $HClO_4$ with and without NPTU at various concentrations. The aim was to evaluate the apparent activation energy and the pre-exponential factor (A) of the corrosion process. This was carried out by studying the temperature dependence of the corrosion current obtained with the potentiodynamic polarisation method. The polarisation exhibits Tafel behaviour. The polarisation curves which are not presented here show that both the anodic and cathodic polarisations decrease upon heating while I_{corr} increases. Several electrochemical parameters were calculated from these curves and the results are summarised in Table 3. I_{corr} increases upon heating both in uninhibited and inhibited solutions. The efficiency of NPTU increases with temperature in the studied temperature range. The fact that (P %) increases with temperature was considered by Ivanov [32] as due to change in the nature of the adsorption mode. The inhibitor is physically adsorbed at lower temperatures, while chemisorption is favoured at higher temperatures (Fig. 10).

Although the adsorption process was sufficiently elucidated by the thermodynamic model, the kinetic model is

Table 2 Impedance parameters and inhibition efficiency for the corrosion of cold rolled steel in 1 M $HClO_4$ containing different concentrations of NPTU, DPTU and PTU at 303 K

	C (M)	R_t (Ω cm^2)	Q (Ω^{-1} cm^{-2} s^n)	n	C_{dl} (μF cm^{-2})	P (%)
Blank		59	21.8×10^{-5}	0.85	103	–
NPTU	5×10^{-5}	208	4.84×10^{-5}	0.87	24.3	71.6
	7.5×10^{-5}	368	4.66×10^{-5}	0.86	24.0	83.9
	1×10^{-4}	450	3.16×10^{-5}	0.84	14.0	86.9
	2.5×10^{-4}	881	2.50×10^{-5}	0.81	10.2	93.3
DPTU	5×10^{-5}	8	18.8×10^{-5}	0.87	71.2	−86.4
	1×10^{-4}	33	5.2×10^{-5}	0.90	25.6	−44.1
	2×10^{-4}	55	3.6×10^{-5}	0.87	14.2	−06.8
	5×10^{-4}	170	7.2×10^{-5}	0.81	25.63	65.3
PTU	1×10^{-4}	7	16.9×10^{-5}	0.89	73.5	−88.1
	2.5×10^{-4}	26	6.6×10^{-5}	0.87	25.5	−55.9
	5×10^{-4}	41	5.5×10^{-5}	0.88	23.9	−30.5
	1×10^{-3}	88	5.4×10^{-5}	0.87	24.3	32.9

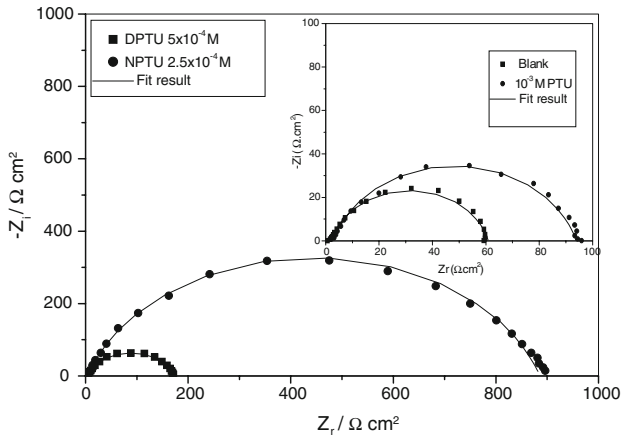

Fig. 8 Curves fitting of EIS data of cold rolled steel in 1 M $HClO_4$ with and without PTU, DPTU and NPTU to Nyquist plots at E_{corr}

another way to explain the mechanism of corrosion inhibition.

The corrosion reaction can be regarded as an Arrhenius process with the rate:

$$\ln I_{corr} = \frac{-E_a}{RT} + \ln A \qquad (6)$$

where E_a represents the apparent activation energy and A is the pre-exponential factor.

Figure 11 gives the Arrhenius plots of the natural logarithm of the corrosion current density vs $\frac{1}{T}$ for 1 M $HClO_4$ with and without NPTU.

E_a and A were calculated by a linear regression method between ln I_{corr} and $\frac{1}{T}$, and the results are shown in Table 4. Linear regression coefficients are close to 1, indicating that steel corrosion in perchloric acid can be understood using the kinetic model.

A close inspection of the data in Table 4 shows that the activation energy is lower in the presence of NPTU. The decrease of E_a with NPTU concentration is typical of the chemisorption process [33, 34].

According to Eq. 6, low values of A and high values of E_a lead to lower corrosion rates. For the present study, E_a is lower in the presence of NPTU. Therefore, the decrease in the steel corrosion rate is decided by the pre-exponential factor A, which reflects the effect of the variation of entropy ΔS_a during activation. It was found that A and consequently ΔS_a significantly decreased with inhibitor concentration reducing the corrosion rate of the cold rolled steel. As a result, the corrosion rate of steel decreased with

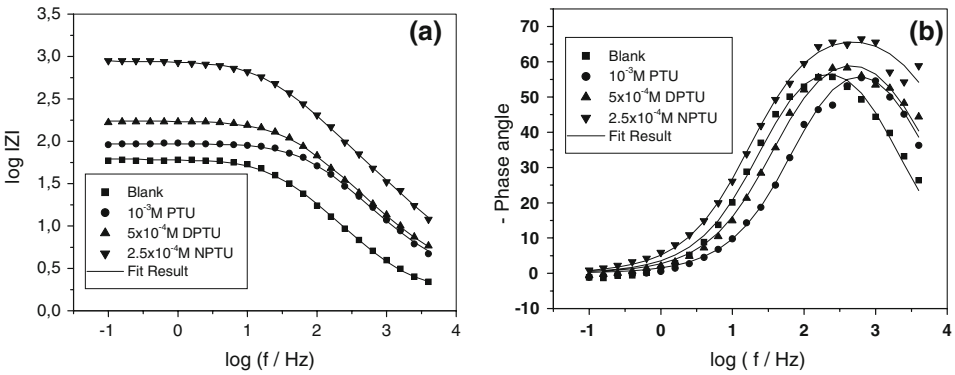

Fig. 9 Bode angle plots for cold rolled steel in 1 M $HClO_4$ with and without PTU, DPTU and NPTU at E_{corr} and at 30 °C (**a**) Bode modulus plots for cold rolled steel in 1 M $HClO_4$ with and without PTU, DPTU and NPTU at E_{corr} and at 30 °C (**b**)

Table 3 Effect of temperature on the inhibition efficiency and electrochemical parameters of the cold rolled steel in 1 M $HClO_4$ with and without NPTU at different concentrations

C (M)	T (K)	$-E_{corr}$ vs SCE (mV)	I_{corr} (μA cm^{-2})	b_c (mV dec^{-1})	P (%)
Blank	298	432	209	173	–
	303	432	489	153	–
	313	435	1,620	168	–
	323	463	4,256	166	–
5×10^{-5}	298	439	44	150	78.9
	303	468	112	145	77.1
	313	452	195	166	87.9
	323	462	319	154	92.5
7.5×10^{-5}	298	462	36	155	82.8
	303	452	57	159	88.3
	313	455	180	159	88.9
	323	432	245	153	94.2
1×10^{-4}	298	442	26	159	87.6
	303	460	38	152	92.2
	313	452	78	152	95.2
	323	447	110	150	97.4
2.5×10^{-4}	298	452	18	150	91.4
	303	452	35	152	92.8
	313	464	56	155	96.5
	323	452	80	159	98.2

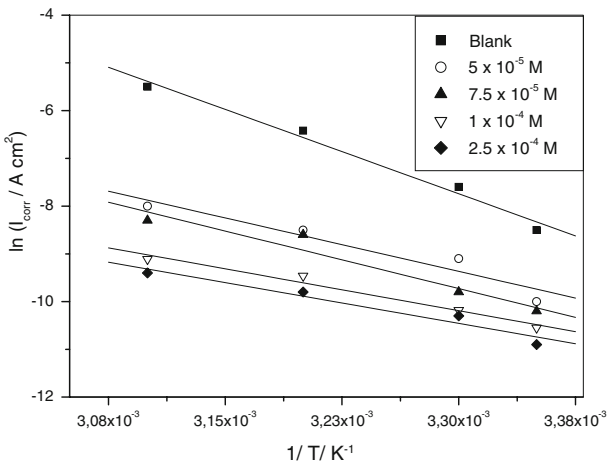

Fig. 10 ln I_{corr} vs $1/T$ for cold rolled steel dissolution in 1 M $HClO_4$ without and with NPTU at various concentrations

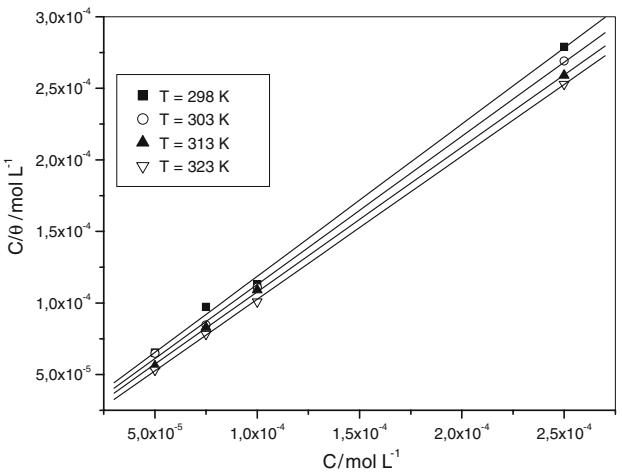

Fig. 11 Curves fitting of the corrosion data of cold rolled steel in the presence of NPTU to Langmuir isotherm at different temperatures

increasing inhibitor concentration. Clearly, the reduction of A is an important factor that determines the corrosion rate of cold rolled steel in 1 M $HClO_4$ in the presence of NPTU.

3.2.2 *The adsorption process*

Assuming that corrosion inhibition was due to the adsorption of NPTU, the degree of metal surface coverage, θ, was calculated from potentiodynamic polarisation measurements using the following relation [35]:

$$\theta = \frac{I_{corr} - I'_{corr}}{I_{corr}} \quad (7)$$

where I_{corr} and I'_{corr} are the current densities for the blank and the inhibited solutions, respectively. This equation is valid under the condition of equal Tafel line slopes, which is satisfied in the present work.

Adsorption of an organic adsorbate at the metal/solution interface can be represented by a substitutional adsorption process between organic molecules in the aqueous solution

Table 4 Some parameters of the linear regression between ln I_{corr} and $1/T$

C (M)	Pre-exponential factor (A cm^{-2})	E_a (kJ mol^{-1})	Linear correlation coefficient
Blank	3.26×10^{13}	97.90	0.992
5×10^{-5}	4.14×10^{6}	61.99	0.961
7.5×10^{-5}	19.32×10^{6}	66.79	0.970
1×10^{-4}	9.14×10^{3}	48.64	0.987
2.5×10^{-4}	4.18×10^{3}	47.34	0.974

$Org_{(sol)}$ and water molecules on the metallic surface $H_2O_{(ads)}$ [36].

$$Org_{(sol)} + xH_2O_{(ads)} \rightleftarrows Org_{(ads)} + xH_2O_{(sol)} \quad (8)$$

where $Org_{(sol)}$ and $Org_{(ads)}$ are the organic molecules in the aqueous solution and those adsorbed on the metallic surface, respectively, $H_2O_{(ads)}$ are water molecules on the metallic surface, x is the size ratio representing the number of water molecules replaced by one molecule of the organic adsorbate.

According to Bockris and Drazic [37], the inhibition mechanism can be explained by the Fe-$(inh)_{ads}$ intermediate reaction:

$$Fe + Inh \rightleftarrows Fe(Inh)_{ads} \rightleftarrows Fe^{n+} + ne + Inh \quad (9)$$

Initially, the amount of $Fe(Inh)_{ads}$ is not sufficient to cover the metal surface, because the inhibitor concentration is insufficient or the adsorption rate is slow. The metal dissolution takes place on sites of the cold rolled steel surface free of $Fe(Inh)_{ads}$. If the inhibitor concentration is high enough, a compact and coherent inhibitor overlayer forms on the steel surface, reducing chemical attack of the metal [38].

When equilibrium is reached in the process described by Eq. 9, it becomes possible to obtain different expressions for the adsorption isotherm plots.

Data of θ were found to fit well with the Langmuir isotherm, given by:

$$\frac{C}{\theta} = \frac{1}{K} + C \quad (10)$$

with

$$K = \frac{1}{55,5}\exp\left(-\frac{\Delta G^{\circ}_{ads}}{RT}\right) \quad (11)$$

C is the concentration of the inhibitor in the bulk solution, K the adsorptive equilibrium constant and ΔG°_{ads} the free energy of adsorption.

According to this isotherm a plot of $\frac{C}{\theta}$ against C should give a straight line with a slope of unity. Figure 11 shows such plots at several temperatures. The plots give straight lines with slopes very close to 1, which confirm the Langmuir adsorption isotherm mechanism. This means that there are no interactions among the adsorbed species [39]. A linear regression calculated by the computer between $\frac{C}{\theta}$ and C gave the parameters listed in Table 5. The adsorption equilibrium constant (K) values increase with increasing temperature. This means that adsorption of NPTU on the steel surface is enhanced at higher temperatures.

Thermodynamic parameters are important in understanding the inhibition mechanism. The values of ΔG°_{ads} at different temperatures were obtained from the values of K and Eq. 11 and plotted against T. This plot is shown in Fig. 12. It should be noted that the entropy change of adsorption $-\Delta S^{\circ}_{ads}$ is the slope of the straight line ΔG°_{ads} vs T according to Eq. 12.

$$\Delta G^{\circ}_{ads} = \Delta H^{\circ}_{ads} - -T\Delta S^{\circ}_{ads} \quad (12)$$

The intercept of the straight line with the y axis gives the heat of adsorption ΔH°_{ads}.

The predicted values of ΔH°_{ads} and ΔS°_{ads} are 47.80 kJmol^{-1} and 287 Jmol^{-1} K^{-1}, respectively. The large negative value of the free energy of adsorption and positive value of the heat adsorption are characteristic of strong adsorption of NPTU. Generally, an exothermic adsorption process means either a physi- or chemisorption mechanism while an endothermic process is attributed unequivocally to a chemisorption process [40]. In the present work, the positive value of ΔH°_{ads} for the adsorption of NPTU indicates that this inhibitor was chemically adsorbed.

Some data are not consistent with the expected adsorption phenomena. It is well known that adsorption is an exothermic phenomenon ($\Delta H^{\circ}_{ads} < 0$) accompanied by a decrease in entropy ΔS°_{ads} [38]. Adsorption of an organic compound on a metal/solution interface is considered as "substitutional adsorption" phenomenon [37]. Thus, the positive value of ΔS_{ads} is attributed to an increase of disorder due to desorption of some water molecules from the iron surface. The positive value of adsorption entropy was also explained by "substitutional adsorption" by Branzoi

Table 5 Some parameters of the linear regression between C/θ and C

Temperature (K)	K (L mol^{-1})	$\Delta G_{ads}{}^{\circ}$ (KJ mol^{-1})	Slope	Linear correlation coefficient
298	8.13×10^{4}	−37.96	1.06	0.9989
303	1.06×10^{5}	−39.25	1.03	0.9995
313	1.49×10^{5}	−41.44	1.01	0.9993
323	3.89×10^{5}	−45.35	1.00	0.9999

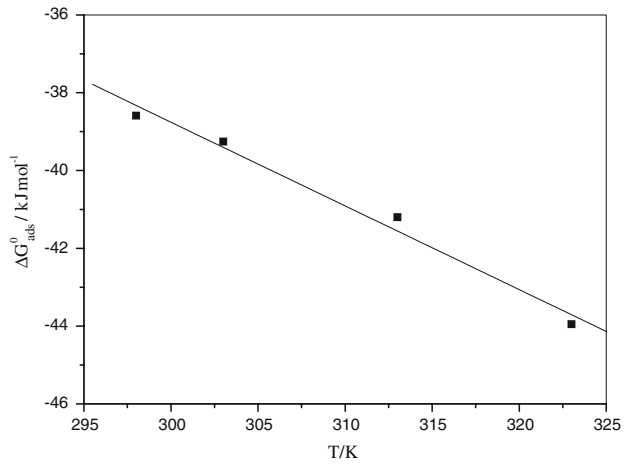

Fig. 12 Free energy of corrosion of cold rolled steel at different temperatures

et al. [38]. These authors studied four surfactants as inhibitors for Armco iron in aqueous solutions of HCl. They found that the four surfactants tested were adsorbed on Armco iron according to the Langmuir isotherm. Such disorder exceeds the ordering phenomenon resulting from the adsorption of only one inhibitor molecule [41]. The positive value of ΔH_{ads} related to "substitutional adsorption" can be attributed to a more positive water desorption enthalpy [42].

Since both adsorption enthalpy and adsorption entropy are positive, the driving force for the adsorption of adsorbate is an increase in entropy during the adsorption process rather that a decrease in enthalpy.

In the present study, chemisorption is clear since the apparent activation energy of corrosion is lower in the presence of NPTU, also because of an increase in inhibition with temperature, a large negative value of ΔG°_{ads} and a positive value of ΔH°_{ads}. According to these arguments, chemisorption of NPTU on the steel surface may take place through donor–acceptor links between π-electrons of the naphthyl group and empty *d*-orbitals of the iron atom. NPTU can also be adsorbed on the metal surface by the interaction between lone pairs of electrons of nitrogen and sulphur atoms of the inhibitor and the metal surface. The covalent bond with the metal is most probably formed between the unpaired electrons of the sulphur atom, which is a better donor of electrons than the nitrogen atom.

4 Conclusions

The following conclusions may be drawn:

- DPTU and PTU act as corrosion stimulators and the acceleration of corrosion of cold rolled steel is higher at lower concentrations.
- The presence of the naphthyl group in the structure of the inhibitor molecule is very beneficial towards inhibition of corrosion of cold rolled steel in 1 M $HClO_4$.
- Addition of NPTU causes inhibition at all concentrations. The inhibitor efficiency increases with its concentration.
- NPTU exhibits both cathodic and anodic inhibition effects but the cathode is preferentially polarised.
- A good agreement is obtained between the polarisation data and electrochemical impedance spectroscopy measurements.
- Adsorption of NPTU onto cold rolled steel varies according to the Langmuir adsorption isotherm.
- Chemisorption of NPTU is evidenced from the apparent activation energy of corrosion, which is lower in the presence of NPTU, the increase in inhibition with temperature, the large negative values of ΔG°_{ads} and the positive value of ΔH°_{ads}.

References

1. Tang L, Li X, Li L, Qing Q, Mu G, Liu G (2005) Mater Chem Phys 94:353
2. Benchekroun K, Delard F, Rameau JJ, El Ghazali A (2002) New J Chem 26:153
3. Bentiss F, Traisnel M, Chaibi N, Mernari B, Vezin H, Lagrenée M (2002) Corros Sci 44:2271
4. Popova A, Sokolova E, Raicheva S, Christov M (2003) Corros Sci 45:33
5. Chetouani A, Hammouti B, Benhadda T, Daoudi M (2005) Appl Surf Sci 249:375
6. Gopi D, Bhuvaneswaran N, Rajeswarai S, Ramadas K (2000) Anti-Corros Meth Mater 47:332
7. Larabi L, Benali O, Harek Y (2007) Mater Lett 61:3287
8. Larabi L, Benali O, Mekelleche SM, Harek Y (2006) J Mater Sci 41:7064
9. Quraishi MA, Ansari FA, Jamal D (2002) Mater Chem Phys 77:687
10. Özcan M, Dehri I, Erbil M (2004) Appl Surf Sci 236:155
11. Hackerman N, Cook EL (2001) J Electrochem Soc 97:3
12. Ahlberg A, Friel M (1989) Electrochim Acta 34:190
13. Agrawal R, Namboodhiri TKG (1990) Corros Sci 39:39
14. Ateya BG, El-Anadouli BE, El-Nizamy FM (1984) Corros Sci 24:497
15. Cheng VL, Ma HY, Chen SH, Yu R, Chen X, Yao ZM (1999) Corros Sci 41:321
16. Raicheva SN, Aleksiev BV, Sokolova EI (1993) Corros Sci 34:343
17. Lawsson MB (1980) Corrosion 36:493
18. Pillai KC, Narayan R (1978) J Electrochem Soc 125:1393
19. Iofa ZA, Batrakov VV, Cho-Ngok-Ba (1964) Electrochim Acta 9:1645
20. Oudar J (1990) Br Corros J 25:21
21. Oldham HG (1989) In: Danami LA (ed) Sulfur containing drugs and related organic compounds, chemistry, biochemistry and toxicology, vol 2 (Part B). Ellis Harwood Limited, Chichester, p 9

22. Stoynov ZB, Grafov BM, Savova-Stoynova B, Elkin VV (1991) Electrochemical impedance. Nauka, Moscow
23. Growcock FB, Jasinski RJ (1989) J Electrochem Soc 136:2310
24. Rammelt U, Reinhard G (1987) Corros Sci 27:373
25. Pang J, Briceno A, Chander S (1990) J Electrochem Soc 137:3447
26. Stoynov Z (1990) Electrochim Acta 35:1493
27. Macdonald JR (1987) J Electroanal Chem 223:233
28. Lopez DA, Simison SN, De Sanchez SR (2003) Electrochim Acta 48:845
29. Popova A, Christov M (2006) Corros Sci 48:3208
30. Wu X, Ma H, Chen S, Xu Z, Sui A (1999) J Electrochem Soc 146:1847
31. Ma H, Chen S, Yin B, Zhao S, Liu X (2003) Corros Sci 45:867
32. Ivanov ES (1986) Inhibitions for metal corrosion in acid media. Metallurgy, Moscow
33. Szauer T, Brandt A (1981) Electrochim Acta 26:1209
34. Foroulis ZA (1990) Proceedings of the 7th European corrosion inhibitors, Ferrara, p 149
35. Gomma GK (1998) Mater Chem Phys 55:131
36. Bockris O'M J, Swinkels DAJ (1964) J Electrochem Soc 111:736
37. Bockris O'M J, Drazic D (1962) Electrochim Acta 7:293
38. Branzoi V, Branzoi F, Baibarac M (2000) Mater Chem Phys 65:288
39. El-Etre AY (2001) Corros Sci 43:1031
40. Durnie W, De Marco R, Kinsella B, Jefferson A (1999) J Electrochem Soc 146:1751
41. Khamis E (1990) Corrosion 46:476
42. Amar H, Benzakour J, Derja A, Villemin D, Moreau B, Braisaz T (2005) Appl Surf Sci 252:6162